On the interactions between carbohydrates and immune cells
Steuten, K.

Chapter 4

Quantification of Siglec unmasking on macrophages

Kas Steuten[1], Bart Straten[2], Johannes J.A. Bakker[1], Geert-Jan Boons[2, 3] & Sander I. van Kasteren[1]

[1] Department of Chemical Biology and Immunology, Leiden Institute of Chemistry, Leiden, The Netherlands
[2] Department of Chemical Biology and Drug Discovery, Utrecht Institute for Pharmaceutical Sciences, and Bijvoet Center for Biomolecular Research, Utrecht University, Utrecht, the Netherlands
[3] Complex Carbohydrate Research Center, University of Georgia, Athens, GA, USA, and Department of Chemistry, University of Georgia, Athens, GA, USA

Manuscript in preparation

4.1 Introduction

In **Chapters 2** and **3**, it was demonstrated that the Glyco-PAINT-APP enables quantitative measurements of mannose binding by C-type lectins in the complex environment of dendritic cells and macrophages. Kinetic parameters such as on-rates, off-rates, and mobility of receptor–ligand complexes were established as key determinants of lectin-dependent cellular functions such as antigen uptake and cross-presentation. These functional outcomes are therefore best understood not simply in terms of receptor abundance or ligand presence, but through the dynamic parameters that govern how a receptor and its ligand interact in real time.

Having defined this kinetic framework for mannose ligands and C-type lectin receptors, we next asked how general these principles are across lectin families, especially in systems where receptor availability is known to be regulated by naturally occurring, endogenous ligands. Among all lectin classes, the sialic acid-binding immunoglobulin-type lectins (Siglecs) of the I-type family represent the most prominent example where receptor accessibility is strongly shaped by cell surface glycosylation. Siglecs recognize a wide variety of glycans containing terminal sialic acid residues. Their signaling can be both pro- and anti-inflammatory through the presence of cytosolic immunoreceptor Tyrosine-based Activation and Inhibition motifs (ITAMs and ITIMs).[1–3] Macrophages represent a cell type that is rich in Siglec expression but the precise dynamics and regulation of Siglec activity on macrophages is unknown. For example, in murine macrophages, expression of Siglec 2, 3, 4, 15, E, G and F has been confirmed on an mRNA transcript level and was critically dependent on macrophage polarization state.[4] In contrast, protein level quantification for the actual presence of these Siglecs on murine macrophages is sparse and has only been confirmed for Siglec-1, E and F.[5–7]

Besides presenting Siglec-receptors, the surface of macrophages is highly decorated with Siglec-ligands that can bind these receptors in *cis*.[4,8] The potential effects of *cis*-binding can be described by estimating the local concentration of sialic acid residues on the macrophage cell surface by quantifying released sialic acid content after sialidase treatment.[9] For example, 20 µg sialic acid was detected from 1 x 10^8 macrophages which is 6.5 x 10^{-16} mol sialic acid per cell[10,11], the surface area of a macrophage is estimated[12] at 380 μm^2 and the thickness of a glycocalyx in culture is estimated at 50 nm.[13] This amounts to a local sialic acid concentration of 30–40 mM at the cell surface, which exceeds SPR-based K_D values for the carbohydrate binding domains of Siglecs themselves that are in the µM to low mM range.[14] Overall, this estimate would mean that, if geometrically possible, the carbohydrate binding pockets of these Siglecs will largely be occupied by these *cis*-ligands and thus be masked as illustrated in **Figure 4.1**.

The phenomenon of Siglec-*cis* binding can in theory have several effects on cell homeostasis that are currently challenging to study. First, it can sequester the *trans*-

sialic acid binding capacity of the receptor, thereby preventing responsiveness to external stimuli. Second, it can lead to *cis*-activation of receptor signaling. In both cases, *cis*-interactions could lead to preorganization of the Siglecs on the cell surface, resulting in apparent multivalent lectin display which in turn can affect the avidity of the *trans*-interactions. This phenomenon was initially reported for the interaction between CD45 and Siglec-2 (CD22) both expressed on B cells.[9,15] Removal (unmasking) of *cis*-ligands by sialidase treatment in these studies was shown to enable *trans*-binding to polymeric, fluorescent $\alpha 2,6$-sialyllactose molecules whereas mock treatment completely abrogated binding of the *trans*-ligand. On macrophages, *cis*-binding was elegantly demonstrated with membrane-anchored *cis*-ligands for Siglec-9.[16] These synthetic *cis*-ligands rely on a lipid anchor that inserts directly into the outermost part of the plasma membrane, positioning the sialylated glycan at the cell surface in a way that mimics the native glycocalyx. Treatment of a macrophage cell line with these synthetic glycolipids in combination with an LPS *trans*-ligand, was shown to inhibit inflammatory cytokine production back to baseline levels. An effect not achieved by the soluble (non-anchored) ligand. These findings motivate the development of Siglec (*cis*-)ligands as potential anti-inflammatory agents.

However, an important gap remains. Although both native and synthetic *cis*-ligands clearly influence Siglec signaling, we still lack quantitative information about how strongly these ligands mask Siglec receptors on the surface of intact macrophages. Masking is a dynamic, cell-state–dependent property that determines whether a Siglec can engage its *trans*-ligand, yet it cannot be inferred from transcript or protein abundance, nor from ligand density alone. In macrophages this uncertainty is amplified by their heterogeneous and not fully defined Siglec expression profile, making it difficult to attribute functional outcomes to a specific receptor. Consequently, a direct and quantitative readout of Siglec availability is needed to understand how *cis*-interactions shape Siglec responsiveness under inflammatory conditions.

To experimentally modulate the extent of Siglec masking, enzymatic and chemical methods that alter cell-surface sialylation have been developed. The most widely used approach is enzymatic removal of terminal sialic acids using exogenous sialidases (Sia), such as those derived from *Clostridium perfringens* or *Vibrio cholerae*, which cleave $\alpha 2,3$-, $\alpha 2,6$- and $\alpha 2,8$-linked sialosides.[17] However, because the glycocalyx is densely packed and heterogeneous in thickness, some sialoglycans may remain sterically shielded from enzymatic access. Metabolic, small molecule, sialyltransferase inhibitors (SI) such as 3FAx-Neu5Ac are therefore used as alternative to suppress *de novo* sialylation and remodel the glycocalyx from within.[18–20]

In this chapter, we quantify the influence of *cis*-interactions on the binding behavior between sialoside ligands and macrophage Siglecs by perturbing sialylation with Sia or SI. Using the Glyco-PAINT-APP optimized for primary cells and a library of fluorophore-labeled sialoside ligands, we assess how sialic acid linkage and multivalency affects Siglec accessibility. We find that unmasking on murine M1

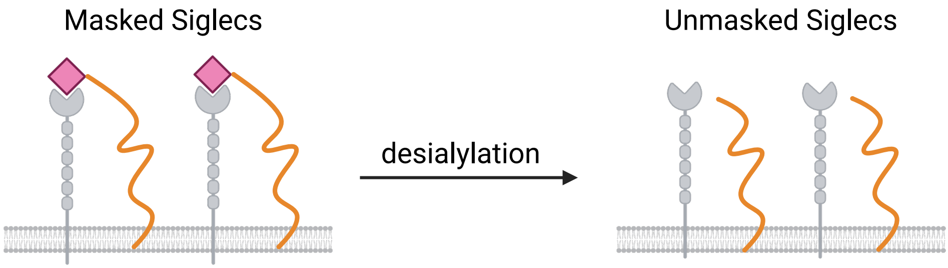

Figure 4.1: Schematic illustration of Siglec unmasking. The sialic acid binding domains of Siglecs can be occupied by *cis*-ligands, thereby preventing *trans*-ligand binding. Subsequent removal of *cis*-ligands can be employed as means for regulation of Siglec signalling activity by the cell.

macrophages is most clearly detected using trivalent $\alpha 2,3$-sialyllactose ligands. Because macrophages have a divergent Siglec expression profile, we cannot assign this behavior to a specific receptor, but the observed ligand-dependent differences provide a functional readout of Siglec accessibility on macrophages.

4.2 Results

4.2.1 Fluorophore-labeled Siglec ligands

Siglec ligands mainly encompass terminal sialic acid residues that are linked through an $\alpha 2,6$ or $\alpha 2,3$ linkage with a, at least for most mammalian glycans, galactose residue.[21,22] These ligands were produced by enzymatic sialylation of a mono- or trivalent lactose-bicyclononyne (BCN), for which the synthesis and characterization is not part of this thesis and will be described elsewhere. The ligands were then subjected to reaction of the BCN strained alkyne with ATTO643-azide. This resulted in fluorescently labeled ligand library (**Figure 4.2**) consisting of $\alpha 2,3$-sialyllactose **(2,3-SL)**, its trimer **(2,3-SL)$_3$**, $\alpha 2,6$-sialyllactose **(2,6-SL)**, and its trimer **(2,6-SL)$_3$**, as well as the non-sialylated lactose control **Lac**.

4.2.2 Quantification of macrophage Siglec binding

Murine macrophages are known to express Siglec-1, E and F and are also rich in cell surface sialylation of which both are dependent on macrophage polarization state.[4,5] We used bone marrow-derived macrophages (BMDMs) to study this binding behavior using the Glyco-PAINT-APP that was described in **Chapter 2** and recorded the binding of 10 nM of monovalent ligands **2,3-SL**, **2,6-SL** and **Lac** for 2000 frames at 50 ms frame rate. The relative, subcellular on-rate, off-rate and the receptor–ligand complex diffusion coefficient were derived using standard 20 x 20 squares analysis settings.

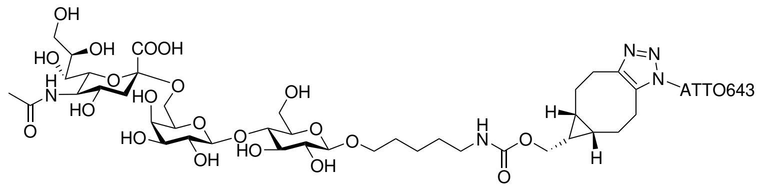

2,6-SL-643

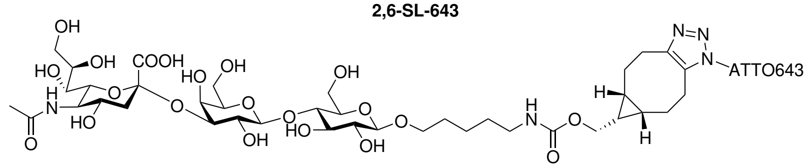

2,3-SL-643

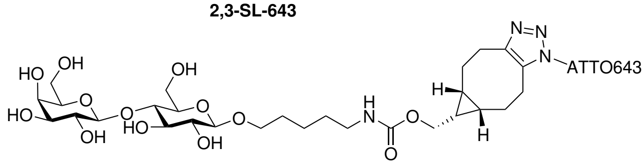

Lac-643

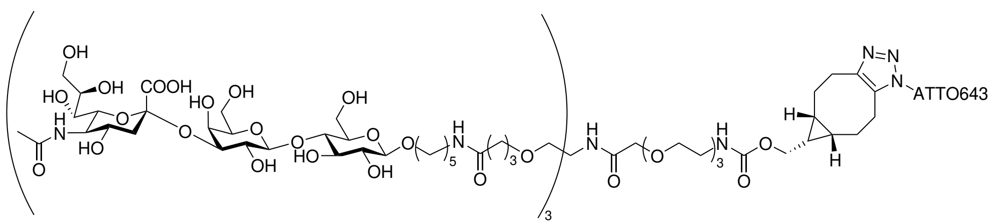

$(2,3\text{-SL})_3$-643

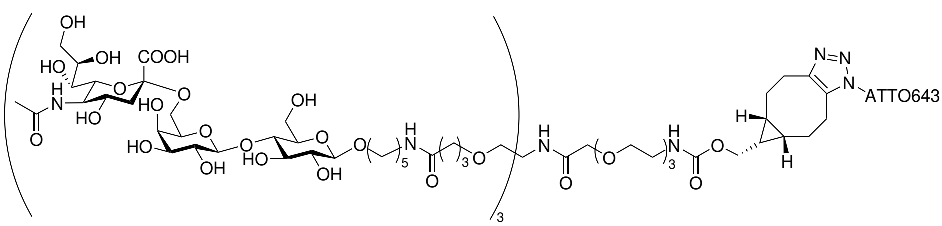

$(2,6\text{-SL})_3$-643

Figure 4.2: Mono- and trivalent ligands to study Siglec binding.

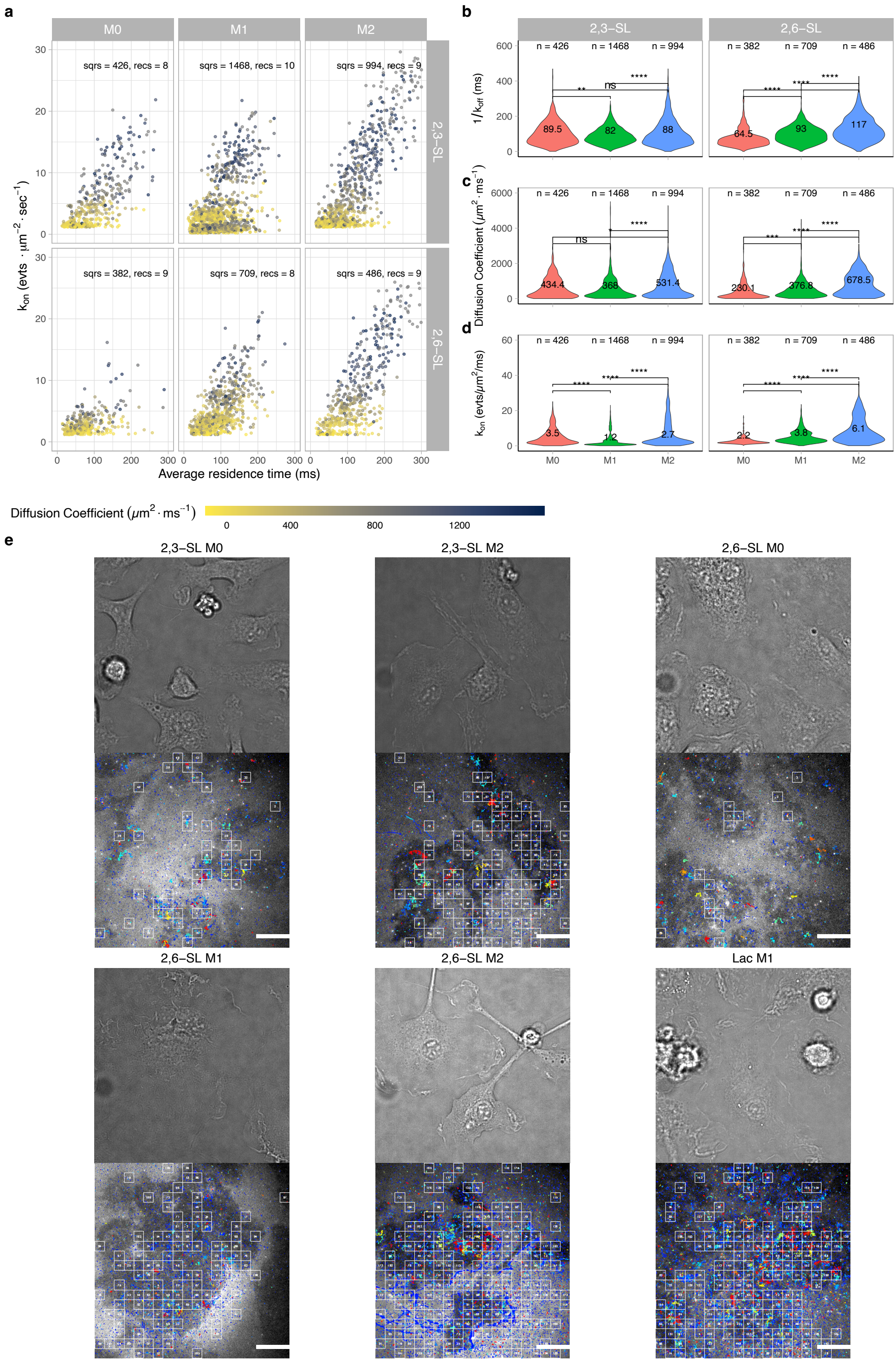

a
M0
M1
M2
2,3–SL
2,6–SL
sqrs = 426, recs = 8
sqrs = 1468, recs = 10
sqrs = 994, recs = 9
sqrs = 382, recs = 9
sqrs = 709, recs = 8
sqrs = 486, recs = 9
k_{on} (evts · μm^{-2} · sec^{-1})
Average residence time (ms)
b
1/k_{off} (ms)
n = 426
n = 1468
n = 994
n = 382
n = 709
n = 486
89.5
82
88
64.5
93
117
ns
c
Diffusion Coefficient ($\mu m^2 \cdot ms^{-1}$)
434.4
368
531.4
230.1
376.8
678.5
d
k_{on} (evts/μm^2/ms)
3.5
1.2
2.7
2.2
3.8
6.1
Diffusion Coefficient ($\mu m^2 \cdot ms^{-1}$)
0
400
800
1200
e
2,3–SL M0
2,3–SL M2
2,6–SL M0
2,6–SL M1
2,6–SL M2
Lac M1

Figure 4.3

Figure 4.3: Polarizing macrophages display unique Siglec-ligand binding profiles. (**a**) Scatterplots displaying on-rate, off-rate and diffusion coefficient for each detected square. (**b-d**) Violinplots for quantitative binding parameters of monovalent sialoside ligands to M0, M1 and M2 macrophages. (**e**) Bright-field images (top row) and tracking overlays (bottom row) for 2,3-SL, 2,6-SL and Lac binding to polarizing macrophages. Glyco-PAINT-APP analysis was performed using a 20×20 grid and filtered with Density_Ratio > 2, R_Squared ≥ 0.9, and Nr_Tracks/Square > 20. Significance was assessed using two-way ANOVA followed by a Tukey post-hoc test. Scalebars in **e** represent 10 µm.

We observed binding of all three ligands to polarizing macrophages (**Figure 4.3e**). Surprisingly, the non-sialylated lactose ligand also showed binding with characteristic parameters that were non-discernible from sialylated ligands as visualised in the scatter- and violinplots displaying the three main binding parameters in **Figure S4.1a, c**. This binding can either be attributed to non-specific interactions or galactose-binding lectins (galectins) that are also present on macrophages.[23] Unique binding profiles for each polarization state as visualized by the scatter and violin distribution plots, could be observed for the sialylated ligands (**Figure 4.3a-d**). The ligand with **2,3-SL** configuration was engaging in areas on M1 macrophages with higher binding parameters as compared to its **2,6-SL** counterpart. While these results confirm binding between the fluorescently labeled *trans*-ligands and the polarizing macrophages, it does not preclude that the observed binding arises through non-specific interactions.

4.2.3 Effects of desialylation on Siglec trans-ligand binding

4

Next, we sought to quantify the contribution of *cis*-ligands expressed on the same cell to the observed *trans*-binding. To do so, M1 cells were subjected to two different desialylation regimens as illustrated in **Figure 4.4b**. In the first regime, macrophages at day 7 of differentiation and after treatment with M1 stimulus were harvested, and whilst in suspension, treated with Sia enzyme for 30 min. Although, this treatment is a commonly applied method for effective sialic acid removal on cancer cells to improve immune recognition[24,25], it is only very scarcely applied on immune cells themselves.[26] In the second regime, macrophages at day 4 of their differentiation trajectory were treated with sialyltransferase inhibitor (SI) 3FAx-Neu5Ac (**Figure 4.4a**) for 3 days. This molecule, which has not been tested on differentiating immune cells before, completely shuts down the cellular synthesis of sialylated epitopes and thereby remodels the glycocalyx from within.

The effect of desialylation using both methods (SI or Sia) was first assessed by staining of M1 macrophages using fluorescently labeled plant lectins that bind to specific glycan epitopes. Peanut Agglutinin (PNA) specifically binds to exposed Galβ1–3GalNAc and *Sambucus Nigra* Agglutinin (SNA) was used to quantify residual sialylated, Neu5Acα2–6Gal/GalNAc, epitopes (**Figure 4.4c, d**). PNA staining of M1 macrophages was found to be more effectively enhanced by Sia treatment than by SI

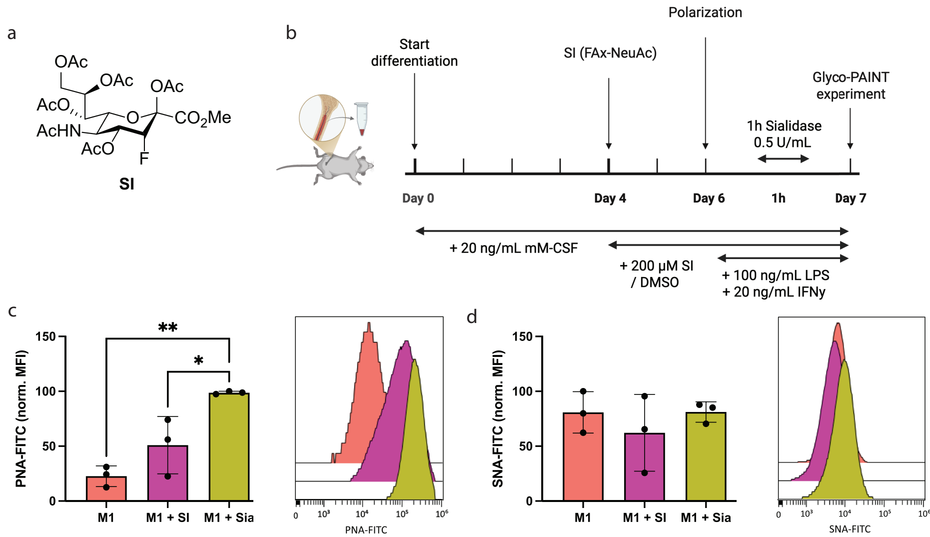

Figure 4.4: Macrophage desialylation using SI or Sia treatment. (**a**) Structure of sialyltransferase inhibitor **3FAx-Neu5Ac** (**b**) Schematic illustration of macrophage differentiation, polarization and desialylation to investigate Sigleccis-binding. (**c, d**) Quantification of cell surface sialic acid expression using plant lectins recognizing unmasked sialoglycans (PNA) or sialic acid residues (SNA) via flow cytometry. Bar graphs represent normalized MFI signals for 3 biological replicates and histograms show representative flow cytometric output. Significance in **b-d** was assessed using two-way ANOVA followed by a Tukey post-hoc test.

in contrast to the reported effects on cancer cell lines.[18,27] SNA signal was largely unaffected for both treatments, suggesting either incomplete removal of sialic acids, or that cross-reactive lectin binding on macrophages obfuscated the effects of sialic acid removal. Further staining data using the $\alpha 2,3$-sialoside-specific *Maackia Amurensis* Lectin (MALII) and human Siglec-9 and 10 Fc-constructs did show a trend towards reduction in binding upon both Sia and SI treatment although significance could not be determined (**Figure S4.2a, b**).

We next attempted to quantify the effects of cell surface desialylation on the *trans*-binding kinetics using Glyco-PAINT-APP. It was found that desialylation by SI treatment only increased the **2,3-SL** on-rate, off-rate and diffusion coefficient as compared to non-treated cells but not for **2,6-SL**. The Sia treatment, in contrast, did not show a uniform increase of these parameters (**Figure 4.5a–c, g**). For the trivalent **(2,3-SL)$_3$** cluster the effect of SI desialylation was even more prominent than its monovalent counterpart (**Figure 4.5d–f, g**) whereas data for Sia treatment of the trivalent clusters binding to M1 macrophages could not be obtained. Of note is that the amount of detected baseline binding events of **(2,3-SL)$_3$** to M1 macrophages was extremely low, only 56 squares over 9 recordings passed selection criteria and are thus visualized in

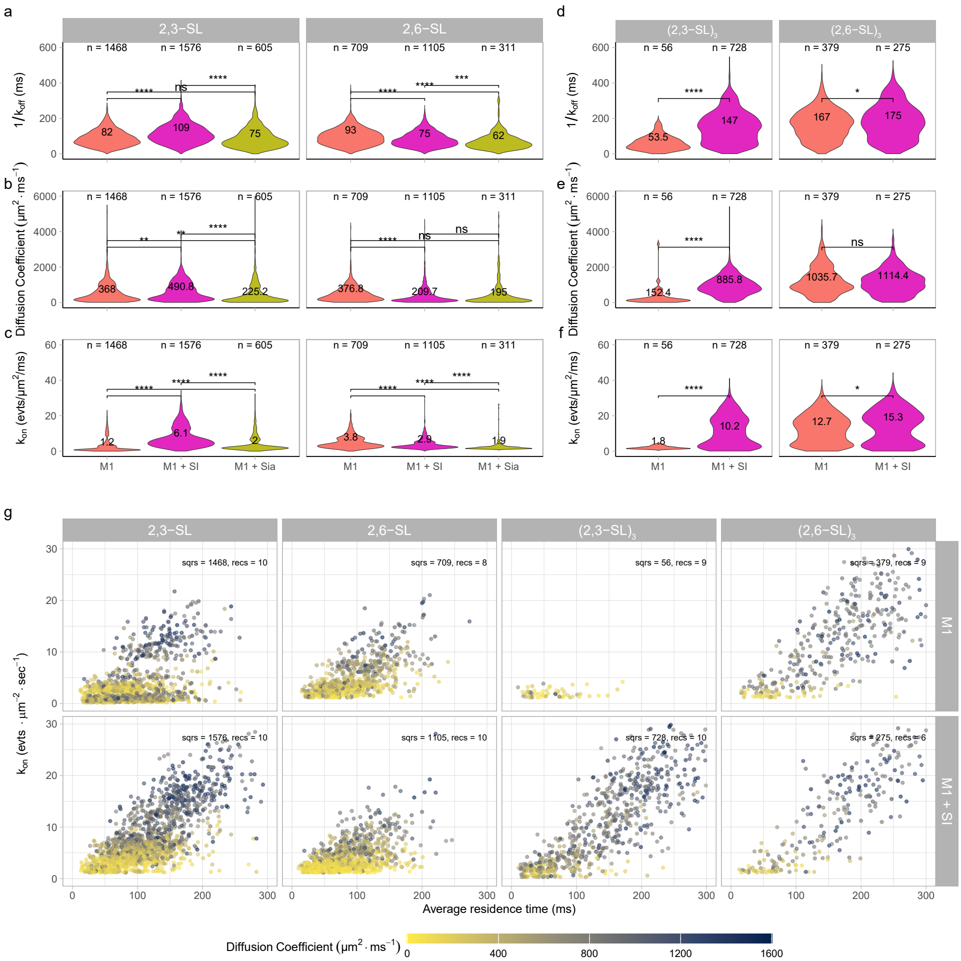

Figure 4.5: Enhanced trans-binding of macrophages after removal of cis-ligands. (**a–c**) Effect of SI or Sia treatment on M1 macrophage binding to monovalent sialyllactose ligands. (**d–f**) Effect of SI treatment on M1 macrophage binding to trivalent ligands. (**g**) Scatterplot display of identical data as in **a–f** indicating enhanced *trans*-ligand binding after SI treatment. n or sqrs, indicates the number of squares from which the data were obtained and recs indicates the number of recordings. Significance across probes was assessed using two-way ANOVA followed by a Tukey post-hoc test. Glyco-PAINT-APP analysis was performed using a 20×20 grid and filtered with Density_Ratio > 2, R_Squared ≥ 0.9, and Nr_Tracks/Square > 20.

the plot. Taken together, these data indicate that single-molecule binding of *trans*-ligands by macrophage Siglecs is enhanced upon removal of cell surface sialic acids by metabolic inhibitor treatment.

4.3 Discussion and conclusion

Siglec unmasking has been proposed as a key regulatory mechanism that shifts Siglec receptors between *cis*-bound, signalling-inhibitory states and *trans*-ligand accessible states. While this concept is supported by biochemical and flow cytometric measurements, direct observation of *cis*- versus *trans*-binding at the level of individual binding events on native primary immune cells has remained technically challenging. Here, we present the first single-molecule quantification of Siglec–glycan interactions on live primary macrophages using the Glyco-PAINT-APP. By employing synthetic fluorescent sialyllactose ligands of defined linkage and valency, we were able to visualize and quantify binding events that reflect the accessibility of Siglec receptors for *trans*-ligands in the context of the endogenous macrophage glycocalyx.

We focused specifically on M1-polarized macrophages due to their upregulation of Siglec-E, an inhibitory Siglec previously implicated in restricting TLR4-driven inflammatory cytokine production.[5] Consistent with this hypothesis, removal of cell-surface sialylation using either acute sialidase treatment or metabolic inhibition of sialyltransferase activity (SI treatment) enhanced binding of both mono- and trivalent **2,3-SL** ligands to M1 macrophages. From these treatments, metabolic suppression of sialylation showed a larger effect on reducing *cis*-occupancy of receptors than enzymatic desialylation. This difference may be explained by regions of the glycocalyx that are sterically protected from Sia access in contrast to SI. While the two desialylation strategies differed in their effectiveness as determined by lectin staining in contrast to malignant cancer cells[19,26–28], it must be emphasized that there is only limited information about the precise binding specificities of these plant lectins towards cells with a, likely, more healthy glycosylation machinery and thus glycocalyx such as the M1 macrophages in this study. To fully determine the extent of sialic acid removal by the two methods, more comprehensive mammalian lectin panels or glycan LC-MS/MS studies will be required.

An important limitation of the current work is that while Siglec-E is a strong candidate for the observed binding profiles, the identity of the specific receptor(s) cannot be conclusively determined. Multiple lectins, including galactose-binding lectins and other Siglecs with overlapping glycan preferences, may contribute to the observed binding events. Definitive assignment will require further studies into absolute Siglec expression levels using quantitative proteomics or transcriptomics. Subsequently, genetic knockouts, blocking antibodies, or engineered overexpression of single Siglec variants in cell lines that lack endogenous expression could aid the assignment of definitive binding partners.

Taken together, our results represent a first step toward the direct single-molecule visualization of Siglec unmasking in a native immune cell context. By quantifying how the macrophage glycome modulates access to Siglec *trans*-ligands, this work provides a foundation for linking glycan remodeling to inhibitory receptor function during macrophage activation. Future studies that combine Glyco-PAINT with genetic or biochemical perturbation of specific Siglecs, as well as functional studies using endogenous or high-affinity Siglec-ligands[29,30], will enable mechanistic dissection of how Siglecs tune inflammatory responses in macrophages at the level of individual receptor–ligand interactions.

4.4 Methods

Acknowledgments We thank the Flow Cytometry Core Facility (FCF) of Leiden University Medical Center (LUMC) in Leiden, The Netherlands for experimental support, use and maintenance of the Sony ID7000. We thank the Animal Research Facility (ARF) at the Leiden University Faculty of Science for mouse breeding and colony management. We thank Nico Meeuwenoord for assistance with glycan cluster purification.

Ethical Statement All animal experiments received approval from the Dutch Central Authority for Scientific Procedures on Animals (CCD) on license number AVD1060020198832 and were conducted in accordance with the European Union Directive 2010/63/EU, recommendation 2007/526/EC.

Mice Male C57Bl/6J mice were purchased from Charles River. The animals were provided with water and food *ad libitum* under a 12:12 day/night cycle. Mice ranging from 8 to 15 weeks old were euthanized by cervical dislocation before harvest of lymphoid organs and/or thigh bones, femur, and tibia.

4.4.1 Cell culture

Bone Marrow-Derived Macrophages (BMDM) Bone marrow (BM) was isolated from femurs, tibias, and thigh bones via centrifugation (1900 rcf, 4.5 min) of scissor-cut bones that were placed in a 1.5 mL tube. The resulting pellet was subjected to red blood cell (RBC) lysis by resuspending in 0.5 mL of ACK lysing buffer (Gibco, A1049201). After 3 min incubation at rt, the suspension was filtered over a 70 µm filter (Falcon, 352350), rinsed with 5 mL PBS and washed once with PBS by 5 min centrifugation at 300 rcf at rt. Thus obtained BM was cryopreserved in 10% DMSO in FCS according to standard methods[31] or directly resuspended at 0.8×10^6 cells/mL

4

in 6-well uncoated culture dishes (Thermo Fisher, 150239) in complete RPMI-1640 (Capricorn, RPMI-A) supplemented with 10% heat-inactivated fetal calf serum (FCS, Gibco, A5670701), penicillin (100 I.U./mL) and streptomycin (50 µg/mL) (Gibco, 15140148), 2 mM GlutaMAX (Gibco, 35050061), 50 µM 2-mercaptoethanol (Gibco, 31350010) and 20 ng/mL M-CSF (Biolegend, 576404) and cultured in a humidified incubator at 37 °C and 5% CO_2. On day 2, 5 mL fresh medium was added and on day 4 medium was aspirated and replenished with 15 mL fresh medium. Cells were used for experiments on day 7 or 8.

4.4.2 Statistical analysis and sample size

Statistical analyses were conducted to compare glycan ligand binding kinetics across probes using the Glyco-PAINT square-based subsampling technology. Subsampling subcellular regions (squares) within fields of view increased the number of independent data points, enhancing statistical power compared to treating entire fields of view or cells as single units. For all Glyco-PAINT experiments at least 3 biological replicates (independent experiments with fresh mouse material) with 3 technical replicates (fields of view per condition) were recorded. For flow cytometry assays at least 3 biological replicates with 2 technical replicates per condition were conducted, unless otherwise indicated. A two-way ANOVA was used to assess differences among probes with respect to kinetic parameters derived from Glyco-PAINT experiments and flow cytometric assays, followed by Tukey's Honest Significant Difference (HSD) test for post-hoc comparisons to control Type I error. Significance is reported as: $p \geq 0.05$ (not significant, ns); $p < 0.05$ (*); $p < 0.01$ (**); $p < 0.001$ (***); and $p < 0.0001$ (****).

4.4.3 Functional Assays

Fluorescent glycan probes Glycan and glycan SLP probes were stored as lyophilized powders at -20 °C. Upon thawing, vials were reconstituted in DMSO and concentration was determined by measurement of absorbance using Nanodrop apparatus with extinction coefficients and eATTO643 = 150.000 $M^{-1}cm^{-1}$ at 665 nm. Small aliquots were stored at -20 °C until use.

BMDM polarization At day 6 cells were polarized by addition of the following cytokines to their media: 20 ng/mL IFN-y (Peprotech, 315-05-100UG) + 100 ng/mL LPS-EB (Invivogen, tlrl-eblps) for M1 or 20 ng/mL IL-4 (Peprotech, 214-14-20UG) for M2 for 16 h.

Desialylation using Sia On day 7 of the differentiation scheme, cells were first washed once with PBS, then incubated with PBS containing 2 mM EDTA at 37 °C for 5 min to release cells, followed by gentle trituration and resuspension in complete medium. For enzymatic desialylation, cells were washed once with pre-warmed PBS and resuspended at 1×10^6 cells per mL in serum-free RPMI. *Clostridium perfringens* neuraminidase (Roche, 11585886001) was added to a final concentration of 500 mU/mL. Cells were incubated for 1 h at 37°C with gentle agitation every 5–10 min. After incubation, cells were washed twice with serum-containing medium and kept on ice for immediate downstream use. Parallel mock-treated control samples were processed in the same manner without the addition of sialidase.

Desialylation using SI For metabolic inhibition of sialylation, cells were cultured for 3 days (starting on day 4 of differentiation scheme) in complete medium supplemented with 200 µM 3FAx-Neu5Ac (MedChemExpress, HY-129746, stock at 50 mM DMSO). Following treatment, cells were washed twice with PBS and used immediately for imaging or flow cytometry. Control cultures received an equivalent final concentration of DMSO without inhibitor.

Lectin and Siglec-Fc Staining Following desialylation or control treatment, $0.1 - 0.5 \times 10^6$ harvested cells were resuspended in PBS containing 0.1% BSA, seeded in a 96 well v-bottom plate and stained on ice for 30 min. PNA-FITC (Vector Labs, FL-1071-10) was used at 5 µg/mL, SNA-FITC (Vector Labs, FL-1301-2) at 2 µg/mL, and MAL-II-biotin (Vector Labs, B-1265-1) at 2 µg/mL followed by streptavidin-BV650 (BioLegend, 405231, 1:500). Siglec-9-Fc (R&D Systems, 1139-SL-050) and Siglec-10-Fc (R&D Systems, 2130-SL-050) were pre-complexed prior to staining by mixing each fusion protein with anti-human Fc-AF647 secondary antibody (Jackson ImmunoResearch) at a 1:2 molar ratio in PBS + 0.1% BSA and incubating for 15 min at room temperature before addition to the cells. After staining, cells were washed twice with cold PBS + 0.1% BSA and analyzed immediately on Sony ID7000 spectral flow cytometer.

4.4.4 Imaging and analysis

Glyco-PAINT optical setup Single-molecule imaging was performed on a Nikon Ti2 N-STORM system equipped with a TIRF module, Z piezo element, perfect focus system for axial drift correction and an OkoLab incubator with temperature and CO_2 controller (37 °C and 5% CO_2) for live-cell imaging. Recordings were acquired using the 647 nm excitation laser (160 mW, 1.9 kW/cm^2). Upon laser excitation, fluorescence was collected by a 100x 1.49 NA oil-immersion objective, passed through a quad-band dichroic mirror (97335 Nikon), and detected by a Hamamatsu ORCA Flash 4.0 CMOS camera with 160 nm pixel size. The signal was collected using the following settings: 512x512 pixel region, no binning, pixel depth 16-bit, exposure time 50 ms, live-cell observation and 2D-STORM (lens out), zoom 1x, lens x0.4, and for live-cell observation at 37 °C the correction collar was set to position 8160.

Acquisition of Glyco-PAINT recordings 1×10^5 BMDM were seeded in 8-well glass-bottomed microscopy slides (Ibidi, 80827) in complete medium. After equilibration in the microscope incubator, fluorescent glycan was added at 10 nM for BMDM experiments. Then, cells were brought into focus using brightfield illumination and 2,000 frames (at 50 ms intervals) were recorded within a single field-of-view at 40–60% of maximum 647 nm laser power using TIRF illumination.

Glyco-PAINT-APP analysis of recordings For the TrackMate processing, a batch file (Experiment Info.csv) containing the experiment metadata and tracking parameters was created. Threshold value was set at 20 by standard unless more than 1,500,000 spots were detected. Recordings were then processed in TrackMate using the 'Run TrackMate Batch' plugin provided by the Glyco-PAINT-APP. Spot detection and tracking by TrackMate was performed as indicated in the batch file using the Simple LAP tracker algorithm with a maximum frame gap of 3, a max linking distance of 0.6 µm and a gap closing max distance of 1.2 µm. Tracks with only two spots were discarded. For the parameter sensitivity analysis, each tracking or spot detection was varied as indicated whilst the others were kept at the aforementioned values (basis scenario).

With the Glyco-PAINT-APP utility 'Generate Squares', a grid of squares was overlaid and kinetic properties for each square were calculated. Default parameters for grid processing are (deviations are mentioned in figure captions): Nr of Squares in row 20, Minimum Tracks to Calculate Tau 20, Min allowable R Squared 0.1, Min Required Density Ratio 2, Maximum Allowable Variability 10 and Neighbour Mode Free. For every recording, a background track count was calculated by averaging the track count of the 40 (10% of the total number of squares) least dense squares. Only squares for which the track count exceeded the Min Required Density Ratio of 2 were considered. For each square, the variability was calculated and only squares for which the variability was less than the Maximum Allowable Variability of 10 were considered. For squares meeting both the Minimum Required Density Ratio and Maximum Allowable Variability criteria, and containing at least the Minimum Tracks to Calculate Tau, kinetic parameters including k_{on}, k_{off} and MSD were calculated as in Riera *et al.*[32], or copied from the TrackMate Tracks table output (for velocity, displacement, and track duration). Summary files were created using the 'Compile Project' utility, creating an 'All Recordings.csv' file, an 'All Squares.csv' file, and an 'All Tracks.csv' file. Statistical analysis and plotting using these merged files was performed using the `ggplot2` package in R.[33,34]

4.4.5 Chemistry Methods

Mono- and trivalent sialyllactose and lactose BCN-conjugated ligands were chemoenzymatically synthesized and characterized by Bart Straten (Utrecht University). For fluorophore conjugation, glycans were dissolved in DMSO at 10 mM and after addition of 0.8 equivalent of ATTO643-azide (Atto-tec GMBH) from a stock concentration of 10 mM in DMSO incubated in a thermoshaker at 37 °C and 300 rpm. Periodically, a 0.5 µL sample was diluted into 39.5 µL of 1:1:1 H_2O:MeCN:tBuOH and analyzed by LC-MS to evaluate reaction progression. The reaction mixture was characterized using electrospray ionization mass spectrometry (ESI-MS) on a Thermo Finnigan LCQ Advantage Max LC-MS instrument with a Surveyor PDA plus UV detector on an analytical C18 column (Phenomenex, 3 µm, 110 Å, 50 mm × 4.6 mm) in combination with buffers A (H_2O), B (MeCN), and C (1% aq. TFA). Quality of crude mixtures was evaluated with a linear gradient of 10-50% B with a constant 10% C over 10 minutes. After full conversion as indicated by LC-MS analysis, the reaction mixture was subjected to size exclusion chromatography over Toyopearl HW-40 size exclusion resin using 150 mM NH_4OAc or 150 mM NH_4HCO_3 (containing 20% MeCN) as the buffer. Fractions showing absorbance above 610 nm were combined and lyophilized.

4.5 Supplementary Figures

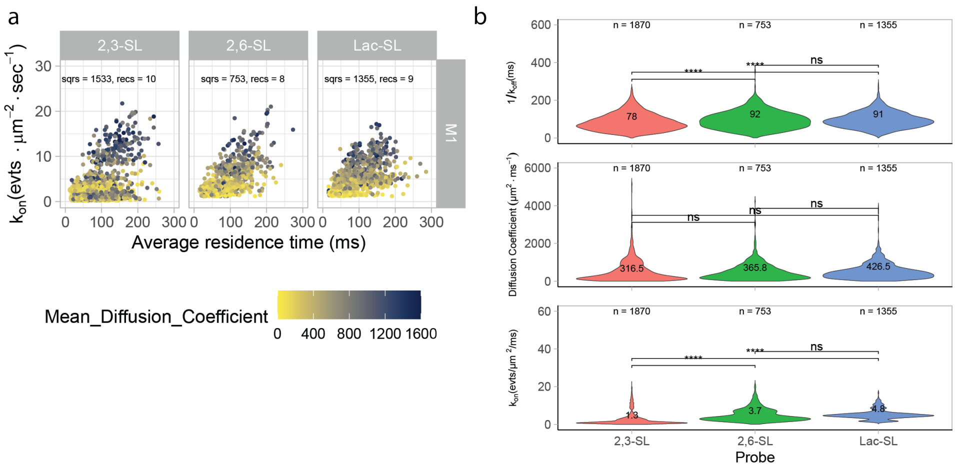

Figure S4.1: Lactose ligand shows equivalent binding to M1 macrophages as sialylactose ligands (a) Scatterplots displaying on-rate, off-rate and mean diffusion coefficient per selected square. (**b**) Identical data as in **a** displayed per individual parameter. Significance across probes was assessed using two-way ANOVA followed by a Tukey post-hoc test. Glyco-PAINT-APP analysis was performed using a 20×20 grid and filtered with Density_Ratio > 2, R_Squared ≥ 0.9, and Nr_Tracks/Square > 20.

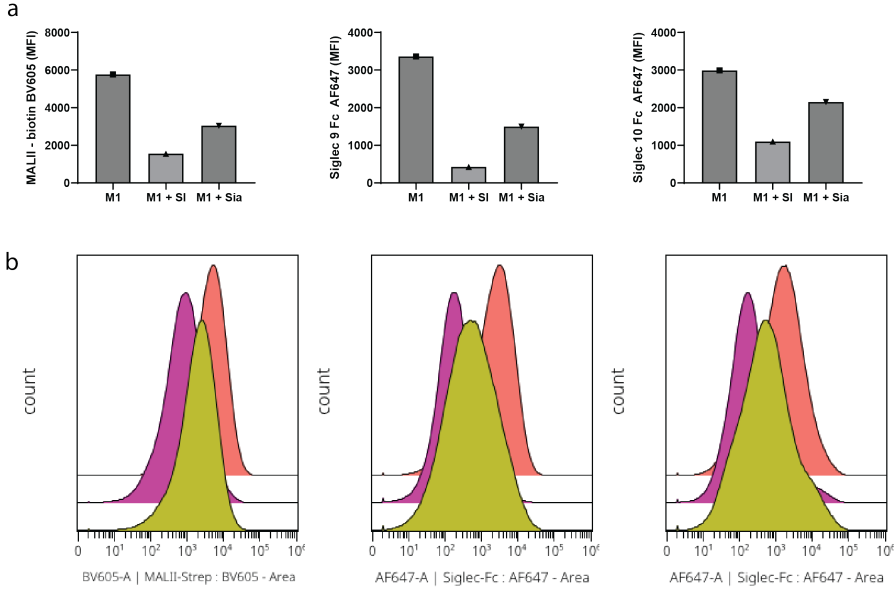

Figure S4.2: Additional quantification of macrophage desialylation (**a**) M1 macrophages treated with either SI or Sia were incubated with MAL-II, Siglec 9-Fc or Siglec 10-Fc followed by either streptavidin or anti-Fc antibodies and staining was quantified using flow cytometry (**b**) Histograms belonging to **a**. Data represent a single biological replicate.

References

(1) Karmakar, J.; Mukherjee, K.; Mandal, C. Siglecs Modulate Activities of Immune Cells Through Positive and Negative Regulation of ROS Generation. *Frontiers in Immunology* **2021**, *12*.

(2) Bornhöfft, K. F.; Goldammer, T.; Rebl, A.; Galuska, S. P. Siglecs: A journey through the evolution of sialic acid-binding immunoglobulin-type lectins. *Developmental & Comparative Immunology* **2018**, *86*, 219–231.

(3) Avril, T.; Freeman, S. D.; Attrill, H.; Clarke, R. G.; Crocker, P. R. Siglec-5 (CD170) Can Mediate Inhibitory Signaling in the Absence of Immunoreceptor Tyrosine-based Inhibitory Motif Phosphorylation *. *Journal of Biological Chemistry* **2005**, *280*, 19843–19851.

(4) Park, D. D.; Chen, J.; Kudelka, M. R.; Jia, N.; Haller, C. A.; Kosaraju, R.; Premji, A. M.; Galizzi, M.; Nairn, A. V.; Moremen, K. W.; Cummings, R. D.; Chaikof, E. L. Resident and elicited murine macrophages differ in expression of their glycomes and glycan-binding proteins. *Cell Chemical Biology* **2021**, *28*, 567–582.e4.

(5) Nagala, M.; McKenzie, E.; Richards, H.; Sharma, R.; Thomson, S.; Mastroeni, P.; Crocker, P. R. Expression of Siglec-E Alters the Proteome of Lipopolysaccharide (LPS)-Activated Macrophages but Does Not Affect LPS-Driven Cytokine Production or Toll-Like Receptor 4 Endocytosis. *Frontiers in Immunology* **2018**, *8*.

REFERENCES

(6) Feng, Y.-h.; Mao, H. Expression and preliminary functional analysis of Siglec-F on mouse macrophages. *Journal of Zhejiang University. Science. B* **2012**, *13*, 386–394.

(7) Uchil, P. D.; Pi, R.; Haugh, K. A.; Ladinsky, M. S.; Ventura, J. D.; Barrett, B. S.; Santiago, M. L.; Bjorkman, P. J.; Kassiotis, G.; Sewald, X.; Mothes, W. A Protective Role for the Lectin CD169/Siglec-1 against a Pathogenic Murine Retrovirus. *Cell Host & Microbe* **2019**, *25*, 87–100.e10.

(8) Macauley, M. S.; Crocker, P. R.; Paulson, J. C. Siglec-mediated regulation of immune cell function in disease. *Nature Reviews. Immunology* **2014**, *14*, 653–666.

(9) Collins, B. E.; Blixt, O.; DeSieno, A. R.; Bovin, N.; Marth, J. D.; Paulson, J. C. Masking of CD22 by cis ligands does not prevent redistribution of CD22 to sites of cell contact. *Proceedings of the National Academy of Sciences* **2004**, *101*, 6104–6109.

(10) Gorczyca, W.; Wieczorek, Z.; Lisowski, J. Cell surface sialic acid affects immunoglobulin binding to macrophages. *FEBS Letters* **1989**, *259*, 99–102.

(11) Kataoka, S.; Kikuchi, T.; Toyota, T. Expression of Receptors for Fc Portion of IgM (Fcμ•R) and Surface Neuraminic Acid on the Human Peripheral Lymphocytes. *The Tohoku Journal of Experimental Medicine* **1985**, *145*, 73–84.

(12) Liu, Y.; Suarez-Arnedo, A.; Riley, L.; Miley, T.; Xia, J.; Segura, T. Spatial confinement modulates macrophage response in microporous annealed particle (MAP) scaffolds. *Advanced healthcare materials* **2023**, *12*, e2300823.

(13) Chappell, D.; Jacob, M.; Paul, O.; Rehm, M.; Welsch, U.; Stoeckelhuber, M.; Conzen, P.; Becker, B. F. The glycocalyx of the human umbilical vein endothelial cell: an impressive structure ex vivo but not in culture. *Circulation Research* **2009**, *104*, 1313–1317.

(14) Blixt, O.; Collins, B. E.; van den Nieuwenhof, I. M.; Crocker, P. R.; Paulson, J. C. Sialoside specificity of the siglec family assessed using novel multivalent probes: identification of potent inhibitors of myelin-associated glycoprotein. *The Journal of Biological Chemistry* **2003**, *278*, 31007–31019.

(15) Razi, N.; Varki, A. Masking and unmasking of the sialic acid-binding lectin activity of CD22 (Siglec-2) on B lymphocytes. *Proceedings of the National Academy of Sciences* **1998**, *95*, 7469–7474.

(16) Delaveris, C. S.; Chiu, S. H.; Riley, N. M.; Bertozzi, C. R. Modulation of immune cell reactivity with cis-binding Siglec agonists. *Proceedings of the National Academy of Sciences* **2021**, *118*, e2012408118.

(17) Juge, N.; Tailford, L.; Owen, C. D. Sialidases from gut bacteria: a mini-review. *Biochemical Society Transactions* **2016**, *44*, 166–175.

(18) Rillahan, C. D.; Antonopoulos, A.; Lefort, C. T.; Sonon, R.; Azadi, P.; Ley, K.; Dell, A.; Haslam, S. M.; Paulson, J. C. Global metabolic inhibitors of sialyl- and fucosyltransferases remodel the glycome. *Nature Chemical Biology* **2012**, *8*, 661–668.

(19) Moons, S. J.; Rossing, E.; Janssen, M. A. C. H.; Heise, T.; Büll, C.; Adema, G. J.; Boltje, T. J. Structure–Activity Relationship of Metabolic Sialic Acid Inhibitors and Labeling Reagents. *ACS Chemical Biology* **2022**, *17*, 590–597.

(20) A. Visser, E.; H. Hornikx, D. L. A.; Rahm, M.; Öztürk, Ö.; Psomiadou, V.; Calzari, M.; Mennen, C.; J. Moons, S.; Jaeger, M.; J. Lefeber, D.; Büll, C.; J. Boltje, T. Investigating the utilization mechanism and kinetics of sialic acid mimetics in mammalian cell lines. *RSC Chemical Biology* **2026**.

(21) *Essentials of Glycobiology*, 4th; Varki, A., Cummings, R. D., Esko, J. D., Stanley, P., Hart, G. W., Aebi, M., Mohnen, D., Kinoshita, T., Packer, N. H., Prestegard, J. H., Schnaar, R. L., Seeberger, P. H., Eds.; Cold Spring Harbor Laboratory Press: Cold Spring Harbor (NY), 2022.

(22) Gonzalez-Gil, A.; Schnaar, R. L. Siglec Ligands. *Cells* **2021**, *10*, 1260.

(23) Henderson, N. C.; Mackinnon, A. C.; Farnworth, S. L.; Kipari, T.; Haslett, C.; Iredale, J. P.; Liu, F.-T.; Hughes, J.; Sethi, T. Galectin-3 Expression and Secretion Links Macrophages to the Promotion of Renal Fibrosis. *The American Journal of Pathology* **2008**, *172*, 288–298.

(24) Büll, C.; Boltje, T. J.; Balneger, N.; Weischer, S. M.; Wassink, M.; van Gemst, J. J.; Bloemendal, V. R.; Boon, L.; van der Vlag, J.; Heise, T.; den Brok, M. H.; Adema, G. J. Sialic Acid Blockade Suppresses Tumor Growth by Enhancing T-cell–Mediated Tumor Immunity. *Cancer Research* **2018**, *78*, 3574–3588.

(25) Gray, M. A.; Stanczak, M. A.; Mantuano, N. R.; Xiao, H.; Pijnenborg, J. F. A.; Malaker, S. A.; Miller, C. L.; Weidenbacher, P. A.; Tanzo, J. T.; Ahn, G.; Woods, E. C.; Läubli, H.; Bertozzi, C. R. Targeted glycan degradation potentiates the anticancer immune response in vivo. *Nature Chemical Biology* **2020**, *16*, 1376–1384.

(26) Silva, M.; Silva, Z.; Marques, G.; Ferro, T.; Gonçalves, M.; Monteiro, M.; van Vliet, S. J.; Mohr, E.; Lino, A. C.; Fernandes, A. R.; Lima, F. A.; van Kooyk, Y.; Matos, T.; Tadokoro, C. E.; Videira, P. A. Sialic acid removal from dendritic cells improves antigen cross-presentation and boosts antitumor immune responses. *Oncotarget* **2016**, *7*, 41053–41066.

(27) Büll, C.; Boltje, T. J.; Wassink, M.; de Graaf, A. M.; van Delft, F. L.; den Brok, M. H.; Adema, G. J. Targeting Aberrant Sialylation in Cancer Cells Using a Fluorinated Sialic Acid Analog Impairs Adhesion, Migration, and In Vivo Tumor Growth. *Molecular Cancer Therapeutics* **2013**, *12*, 1935–1946.

(28) Grabenstein, S.; Barnard, K. N.; Anim, M.; Armoo, A.; Weichert, W. S.; Bertozzi, C. R.; Parrish, C. R.; Willand-Charnley, R. Deacetylated sialic acids modulates immune mediated cytotoxicity via the sialic acid-Siglec pathway. *Glycobiology* **2021**, *31*, 1279–1294.

(29) Prescher, H.; Frank, M.; Gütgemann, S.; Kuhfeldt, E.; Schweizer, A.; Nitschke, L.; Watzl, C.; Brossmer, R. Design, Synthesis, and Biological Evaluation of Small, High-Affinity Siglec-7 Ligands: Toward Novel Inhibitors of Cancer Immune Evasion. *Journal of Medicinal Chemistry* **2017**, *60*, 941–956.

(30) Hong, S.; Yu, C.; Rodrigues, E.; Shi, Y.; Chen, H.; Wang, P.; Chapla, D. G.; Gao, T.; Zhuang, R.; Moremen, K. W.; Paulson, J. C.; Macauley, M. S.; Wu, P. Modulation of Siglec-7 Signaling Via In Situ-Created High-Affinity cis-Ligands. *ACS Central Science* **2021**, *7*, 1338–1346.

(31) Marim, F. M.; Silveira, T. N.; Jr, D. S. L.; Zamboni, D. S. A Method for Generation of Bone Marrow-Derived Macrophages from Cryopreserved Mouse Bone Marrow Cells. *PLOS ONE* **2010**, *5*, e15263.

(32) Riera, R.; Hogervorst, T. P.; Doelman, W.; Ni, Y.; Pujals, S.; Bolli, E.; Codée, J. D. C.; van Kasteren, S. I.; Albertazzi, L. Single-molecule imaging of glycan–lectin interactions on cells with Glyco-PAINT. *Nature Chemical Biology* **2021**, *17*, 1281–1288.

(33) R Core Team, *R: A Language and Environment for Statistical Computing*; R Foundation for Statistical Computing: Vienna, Austria, 2023.

(34) Wickham, H., *ggplot2: Elegant Graphics for Data Analysis*; Springer-Verlag New York: 2016.